Phase diagram of the one-dimensional extended Hubbard model with attractive and/or repulsive interactions at quarter filling

Karlo Penc*
Institut de Physique, Université de Neuchâtel, 1 Rue Breguet, CH-2000 Neuchâtel, Switzerland

Frédéric Mila
Laboratoire de Physique Quantique, Université Paul Sabatier, 31062 Toulouse, France
(Received 29 November 1993)

We study the phase diagram of the one-dimensional U-V model at quarter filling in the most general case where the on-site and first-neighbor interactions U and V can be both attractive and repulsive. The results have been obtained using exact diagonalization of small clusters and variational techniques, as well as exact results in various limits. We have analyzed four properties of the ground state: (i) whether it is insulating or metallic; (ii) whether it is homogeneous or phase separated; (iii) whether it has a spin gap; (iv) whether it has dominant superconducting fluctuations. With eight phases, the resulting phase diagram is unexpectedly rich. The four phases not found in the weak coupling limit are: (i) an insulating phase when U and V are large enough; (ii) a region of phase separation when V is attractive; (iii) another region of phase separation when V is large enough and U small; (iv) a region with dominant superconducting fluctuations when V is intermediate and U small. The actual nature of this last phase, which has pairs but no spin gap, is not fully clear yet.

I. INTRODUCTION

The phase diagram of one-dimensional models of correlated fermions is well understood in the limit of weak interactions. In that case, the model can be mapped using perturbation theory and a cutoff procedure onto the so-called Fermi gas model (also referred to as g-ology), a model whose properties are well established.[1,2] In the opposite limit of strong interactions, perturbation theory cannot be used to perform such a mapping, and the determination of the phase diagram is in most cases a very difficult problem. The exceptions are models that have an exact solution, like for instance the one-dimensional (1D) Hubbard model.[3] In the case of that particular model, no qualitatively new physics appears in going from weak to strong coupling. So it is legitimate to wonder whether there is a real need of studying the strong coupling regime of more complicated models. We believe this is the case for at least two reasons. First, real materials whose properties are of one-dimensional character are not necessarily in the weak-coupling regime, and understanding their electronic properties requires some knowledge of the properties of intermediate or strong coupling models. A very important example is the case of the organic conductors of the $(TMTSF)_2X$ family, where TMTSF=tetramethyltetraselenafulvalene. In a large temperature range, they exhibit low-energy properties that have a clear one-dimensional character and that are compatible with the Luttinger-liquid picture[4–6] if the exponent α defined by $N(\omega) - N(\omega_f) \propto \Theta(\omega_f - \omega)(\omega - \omega_f)^\alpha$ is slightly larger than 1, where $N(\omega)$ is the density of states. Such an exponent is impossible to get with weak interactions which always yield $\alpha \ll 1$. The only hope to reach such a value is to turn to strong coupling models. Let us note that the Hubbard model is not able either to reproduce such an exponent: α is at most equal to 1/8, a value attained in the very strong coupling limit $U = +\infty$.[6,7]

Second, it has been known for a long time that the strong coupling regime of extensions of the Hubbard model can give rise to new physics. For example, it was first shown by Ovchinnikov[8] that adding a repulsion term V between nearest neighbors to the Hubbard model yields a metal-insulator transition for $V = 2t$ when U is infinite in the case of quarter filling, a phenomena not observed in the weak coupling regime of the same model. More generally, commensurability between the number of particles and the number of sites can give rise to a metal-insulator transition in the weak-coupling limit only at half filling, while this effect can in principle occur for any commensurate filling if strong interactions are considered.

In this paper, we concentrate on the properties of the U-V model at quarter filling defined by the Hamiltonian

$$H = -t \sum_{i,\sigma} (c^\dagger_{i\sigma} c_{i+1\sigma} + \text{H.c.}) + U \sum_i n_{i\uparrow} n_{i\downarrow} + V \sum_i n_i n_{i+1}, \quad (1)$$

where U and V are allowed to take positive or negative values, i.e., to describe repulsive or attractive interactions. An account of the properties of this model in the case of repulsive interactions has already been given.[9] Unexpected results showed up in the limit U small, V large, and an extension of the model to negative couplings was clearly needed in order to clarify the properties of the model in the large V limit.

Before we start the description of the phase diagram of the model of Eq. (1), let us recall what is meant by phase

diagram in the context of one-dimensional systems.[1,2] In general, phases are distinguished by some kind of long-range order. If one sticks to that definition, there are only three possibilities for 1D systems: (i) insulating phase if there is a gap Δ_c in the charge sector; (ii) metallic phase if there is no gap in the charge sector; (iii) phase separation if the ground state is not homogenous. Any kind of magnetic or superconducting long-range order is forbidden in 1D because of quantum fluctuations. However, the correlation functions do not decay exponentially but as power laws, that is very slowly, and it is useful to distinguish regions in the metallic phase according to the correlation function that decays most slowly. This is useful because any infinitesimal coupling between the chains, that will be present in real materials, will introduce long-range order associated with that correlation function. According to g-ology, there are at least four different types of metallic phases that can be distinguished by the value of the critical exponent K_ρ (to be defined below), and by the presence or absence of a gap Δ_s in the spin sector. Quite generally, superconducting fluctuations dominate if $K_\rho > 1$, while charge and spin density fluctuations dominate if $K_\rho < 1$. Now, if there is no spin gap, triplet and singlet pairing correlation functions on the one hand, charge density and spin density correlation functions on the other hand, have the same power law behavior, and one has to look at logarithmic corrections to see that triplet pairing and spin density fluctuations dominate over singlet and charge density fluctuations, respectively. If there is a spin gap, triplet pairing and spin density fluctuations decay exponentially, and singlet pairing and charge density will be the dominant fluctuations. To summarize, one can expect to find six types of phases: (1) metallic with dominant spin density fluctuations if $\Delta_c = \Delta_s = 0$ and $K_\rho < 1$; (2) metallic with dominant triplet pairing fluctuations if $\Delta_c = \Delta_s = 0$ and $K_\rho > 1$; (3) metallic with dominant charge density fluctuations if $\Delta_c = 0$, $\Delta_s > 0$ and $K_\rho < 1$; (4) metallic with dominant singlet pairing fluctuations if $\Delta_c = 0$, $\Delta_s > 0$ and $K_\rho > 1$; (5) insulating if $\Delta_c > 0$; (6) Phase separation if the compressibility of the homogenous phase is negative.

The paper is organized as follows. In Sec. II, we summarize the results one can get from g-ology in the weak coupling regime. In Sec. III, we present the general phase diagram and provide detailed explanations on how the various boundaries have been determined. In Sec. IV, we give some exact results that can be obtained in the $V = +\infty$ case and that are useful to check the numerical determination of the boundaries. Finally, a detailed discussion of the large V, small U case is given in Sec. V. This includes a derivation of an effective Hamiltonian in that limit and some numerical results of flux quantization used to analyze the presence of pairs in the ground state.

II. THE WEAK-COUPLING PHASE DIAGRAM

When the interaction terms are small compared to the Fermi velocity, one can rewrite the Hamiltonian in momentum representation and map it onto the g-ology model. For the Hamiltonian of the Eq. (1) at quarter filling the g parameters are given by

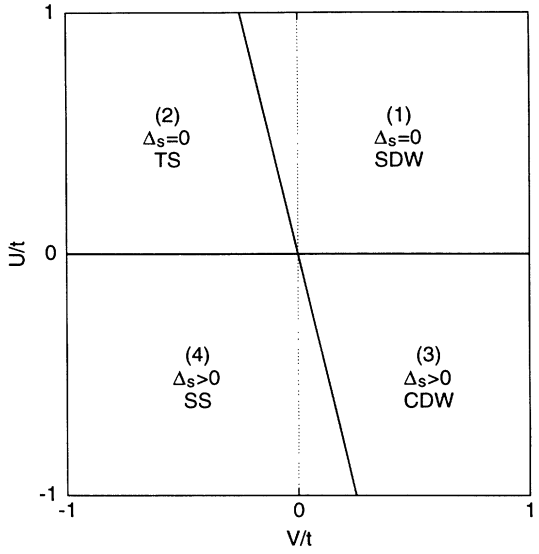

FIG. 1. Phase diagram in the weak coupling limit.

$$\begin{aligned} g_1 &= U + 2V\cos 2k_F a = U, \\ g_2 &= U + 2V, \\ g_3 &= 0, \\ g_{4\perp} &= U + 2V, \\ g_{4\parallel} &= 2V. \end{aligned} \tag{2}$$

The coupling g_3 is equal to zero because we are away from half filling.

The schematic phase diagram for the quarter-filled model is presented in Fig. 1, where the different phases are numbered from (1) to (4). If $U > 0$ ($g_1 > 0$), we scale to the Tomonaga-Luttinger model. From the scaling invariant $2g_2 - g_1$ the fixed-point value of the forward scattering is $g_2^* = U/2 + 2V$. For $U > -V/4$ there are strong charge or spin density wave fluctuations [region numbered by (1) in Fig. 1] and for $U < -V/4$ ($g_2^* < 0$) large superconducting fluctuations are present [phase (2)]. On the other hand, if $U < 0$ ($g_1 < 0$), we scale to strong coupling. We know from the solution along the Luther-Emery line that there is a gap in the spin spectrum, and charge density (3) or superconducting fluctuations (4) are favored when $U + V/4$ is positive or negative, respectively.

III. THE GENERAL PHASE DIAGRAM

To determine the general phase diagram, we must calculate the charge gap Δ_c, the spin gap Δ_s, the critical exponent K_ρ, and the compressibility κ.

A. The charge gap

Let us start with the charge gap. It is given by $\Delta_c = \lim_{L\to+\infty} \Delta(L; L/2)$, where $\Delta(L; N)$ is defined by

$$\Delta(L;N) = E_0(L;N+1) + E_0(L;N-1) - 2E_0(L;N). \tag{3}$$

In that expression, $E_0(L;M)$ is the ground-state energy of M particles on L sites and can be obtained by exact diagonalization of small clusters using Lanczos algorithm. Such a procedure has been used by Spronken *et al.*[10] for the case of spinless fermions with nearest-neighbor repulsion, and the critical value $V_c = 2t$ could be reproduced quite accurately by fitting $\Delta(L;N)$ with polynomials of $1/L$. In our case, the Hilbert space is much larger, and we have results for three sizes only (L=8,12,16). So, we cannot expect a very good accuracy. In fact, we could not get meaningful results by fitting these three values with $A+B/L+C/L^2$. However, fitting any pair of values with $A+B/L$ gives reasonable results that do not depend too much on the pair chosen to do the fit. Besides, as far as the large U case is concerned, the best result is obtained by fitting the results for $L = 8$ and 16. This is probably due to the fact that the 12-site system is quite different from the other two: To get smooth results as a function of L, one must choose the boundary conditions so that k_F is one of the allowed k values, that is periodic ones for 8 and 16 sites, and antiperiodic ones for 12 sites.[10] It turns out that the insulating region is confined to the $U > 0, V > 0$ sector. The resulting boundary goes from $(U,V) = (+\infty, 2t)$ to $(U,V) = (4t, +\infty)$. The first point is just the exact result obtained by Ovchinnikov some years ago,[8] while the second one is an exact result that we derive in Sec. III.

B. The spin gap

We now turn to the spin gap. It corresponds to the energy needed to make a triplet excitation from the singlet ground state and can be calculated as $\Delta_s = \lim_{L\to+\infty} \Delta_s(L;L/2)$, where $\Delta_s(L;N)$ is defined by

$$\Delta_s(L;N) = E_0(L;N;S^z=1) - E_0(L;N;S^z=0). \tag{4}$$

$E_0(L;N;S^z=s)$ is the ground-state energy of a system of N particles on L sites in the sector $S^z = s$. As for the charge gap, and presumably for the same reasons, the best way of extrapolating the finite-size results is to do a linear fit of the results obtained for $L = 8$ and $L = 16$. The resulting boundary goes through the point $(U,V) = (0,0)$ with a slope parallel to the V axis, as it should according to the weak-coupling results. Besides, our numerical results seem to indicate that it ends at the point $(U,V) = (-4t, +\infty)$, a result we also prove in Sec. III.

C. The critical exponents

The nature of the ground-state and of the low-lying excitations when there is no charge gap is a very difficult problem. In principle, one can get the excitation spectrum for finite systems and see what the elementary excitations are. Hopelessly, with the sizes that are available, it is not possible to distinguish any structure that will remain in the thermodynamic limit with any degree of confidence. The only thing that is possible at the moment is to assume that the spectrum has a certain structure and to check if this is compatible with the finite-size results. In the case of 1D systems, we know that, in the weak coupling regime, the metallic phase is a Luttinger liquid. Noting that this is also true for the Hubbard model for all U, it is a reasonable hypothesis to assume that this is still the case for the model of Eq. (1). Then one can deduce the parameters of the model from the low-energy part of the spectrum[11,12] obtained numerically for small clusters, and check *a posteriori* if these parameters are consistent with the hypothesis. One can estimate the ratio u_ρ/K_ρ by using its relation to the compressibility κ

$$\frac{\pi}{2}\frac{u_\rho}{K_\rho} = \frac{1}{n^2\kappa}, \tag{5}$$

$$\kappa = \frac{L}{N^2}\left(\frac{E_0(L;N+2) + E_0(L;N-2) - 2E_0(L;N)}{4}\right)^{-1}. \tag{6}$$

Equation (6) is the finite-size approximation to the compressibility, $E_0(L;N)$ being the ground-state energy calculated with suitable boundary conditions. The charge velocity can be obtained from the low-energy spectrum as

$$u_\rho = [E_1(L;L/2;S=0) - E_0(L;L/2)]/(2\pi/L), \tag{7}$$

where $E_1(L;L/2;S=0)$ is the energy of the first singlet excited state. The analysis of the t-J model by Ogata *et al.*[13] was based on these equations.

In our study, we have also used another relation that holds for Luttinger liquid, namely

$$\sigma_0 = 2u_\rho K_\rho, \tag{8}$$

where σ_0 is the weight of the Drude peak of the conductivity. In 1D systems, σ_0 can be obtained simply from[14–16]

$$\sigma_0 = \frac{\pi}{L}\left.\frac{\partial^2 E_0(\phi)}{\partial\phi^2}\right|_{\phi=0}, \tag{9}$$

where $E_0(\phi)$ is the ground-state energy as a function of a phase ϕ due to a flux $\Phi = L\phi$ through the ring. Equations (5)–(9) provide us with three independent conditions on u_ρ and K_ρ. This is very useful for several reasons. First, the conductivity is much simpler to evaluate numerically than the compressibility, which involves systems with $N+2$ particles. Besides, we have good reasons to believe that Eq. (6) does not give a reliable estimate of the compressibility when V is large, and it is important to be able to determine K_ρ without its help.

It turns out that there are two disconnected curves $K_\rho = 1$. One curve goes through the point $(U,V) = (0,0)$ and corresponds to the boundary found in the weak-

coupling case. The slope found at $(U,V) = (0,0)$ in our numerical determination of this boundary is in good agreement with the one predicted by the weak-coupling analysis. There is however another line $K_\rho = 1$ in the small U, large V region which has no counterpart in the weak-coupling case. This line goes through the point $(U,V) = (0, \sim 8t)$ and seems to extend toward the points $(4t, +\infty)$ and $(-4t, +\infty)$. It is not possible to decide whether these points really correspond to the limits of this line on the basis of our numerical results however: The estimate of K_ρ becomes unreliable when V gets very large. As we could not get exact results about K_ρ in the $V = +\infty$ case, this behavior remains a conjecture. Our numerical results also suggest that this line lies entirely in the region where there is no spin gap, although we cannot be totally sure either.

To complete the analysis of the metallic phase, we now have to check the validity of the hypothesis we made about the excitations of the system, namely that they are those of a Luttinger liquid. We can check this hypothesis in two independent ways. First, we can use the consistency of the three equations used to determine K_ρ and u_ρ to check the assumption that the system is a Luttinger liquid: Equations (5) and (6) and (8) and (9) are typical of Luttinger liquids and will be violated if we have an instability to another phase [e.g., charge density wave (CDW) insulator]. A convenient way to measure the consistency of the three conditions is to calculate the ratio $\sigma_0/\pi n^2 \kappa u_\rho^2$ which equals 1 for a Luttinger liquid. We have performed a systematic evaluation of this ratio along lines in the (U,V) plane. In the region where Eq. (7) can be used, i.e., when V is not too large, we found that, to a good accuracy, this ratio equals 1 in the metallic phase, that it drops rapidly when one enters the insulating phase, and that the transition point was in good agreement with our previous determination of the phase boundary.

Another way to check that we have a Luttinger liquid is to extract the central charge from the finite-size scaling of the ground-state energy density[12]

$$e_0(L) = e_0(+\infty) - \frac{\pi(u_\rho + u_\sigma)}{6L^2} c + o(1/L^2). \qquad (10)$$

u_σ was obtained from

$$u_\sigma = [E_1(L; L/2; S^z = 1) - E_0(L; L/2)]/(2\pi/L), \quad (11)$$

where $E_1(L; L/2; S^z = 1)$ is the energy of the first excited state in the sector $S^z = 1$. Comparing our results for L=8, 12, and 16, we found that this scaling form was accurate except when V is too large, and that the central charge c determined in this way equals 1 within 2%, in good agreement with the exact value $c = 1$ for Luttinger liquids.

To summarize, we have been able to prove numerically that, when it is metallic, the system is a Luttinger liquid, except when V is large, in which case finite-size effects prevent us from checking this hypothesis.

D. The compressibility

Finally, we must calculate the compressibility to determine whether the homogenous phases considered so far are stable against phase separation. Reliable estimates of the compressibility are very difficult to extract in the interesting regions where it changes signs due to huge finite-size effects. So we had to turn to variational techniques to estimate this quantity. More precisely, we have used an extended Gutzwiller ansatz to calculate the ground-state energy as a function of density. Details can be found in Appendix A. As for K_ρ, we found two disconnected lines of phase separation. One is entirely located in the $V < 0$ half plane and goes from $(U,V) = (+\infty, -t)$ to $(U,V) = (-\infty, 0)$. The first point is exactly the value obtained by other authors from the mapping of that model onto the anisotropic XXZ Heisenberg model in the limit $U = +\infty$ (see, e.g., Ref. 11). The other limit is not surprising either: For $U = -\infty$, the ground state is a collection of static pairs. If $V > 0$, they will tend to stay apart, while if $V < 0$, they will gain energy by staying as close as possible. The other phase separation line lies in the small U, large V region. It goes through the point $(U,V) = (0, 15t)$ and apparently extends toward the points $(U,V) = (4t, +\infty)$ and $(U,V) = (-4t, +\infty)$. In fact, we will prove in the next section that these points lie on the boundary. So this variational approach to the determination of phase separation looks quite reliable.

E. The phase diagram

The resulting phase diagram is shown in Fig. 2. It contains eight different phases. The physical origins of most of them is already clear. The insulating phase is a spin density wave that occurs because of commensurability and was discussed in some detail before.[9] The nature of the ground state in the $V < 0$ phase separation region is also quite easy to guess. If U is large enough, one will have a region of density 1 with one particle per site and an empty region, while if U is small or negative, one will have a region of density 2 and an empty region. The limit between the two cases is presumably the continuation of the $\Delta_s = 0$ line, although we have not tried to determine it. Besides, four of the metallic phases have a weak coupling counterpart, and they simply correspond to cases (1)–(4) of the Introduction. The two phases that occur when V is large and U is small are not so easy to account for however. The rest of the paper is devoted to a detailed discussion of this region. In particular, the origin of the phase separation will be clear from the solution of the $V = +\infty$ case.

IV. THE $V = +\infty$ CASE

In this limit a pair of electrons on the same site cannot be broken, since it would mean hopping to the nearest site at an energy cost of $V = +\infty$. The treatment of the model in this limit is greatly simplified by this fact. The unpaired fermions can move in the regions located between pairs. Moreover, unpaired fermions cannot be on neighboring sites, so the spin is not relevant and its contribution is only to increase the degeneracy of the energy levels. In Appendix B an effective Hamiltonian

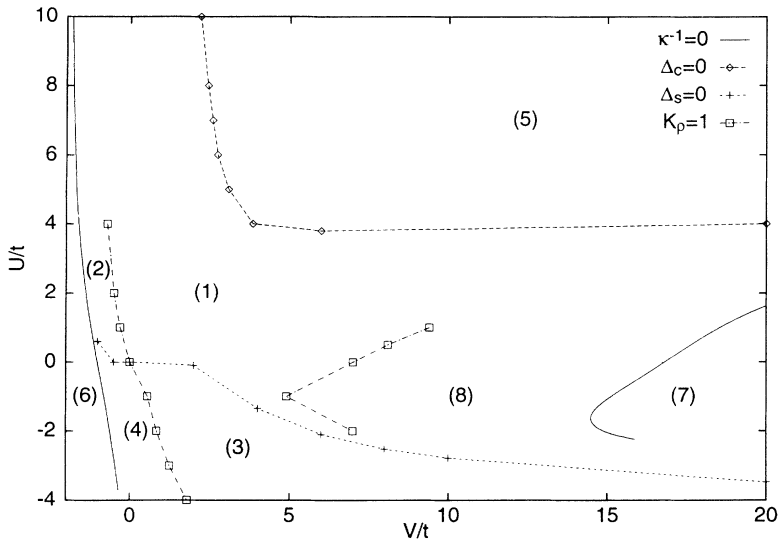

FIG. 2. Phase diagram of the U-V model at quarter filling. The nature of the various phases is discussed in the main text.

is derived for the case where the V is much larger than U and t, and the $V = +\infty$ case is described by the H_0 [Eq.(B5)].

The eigenstates can be classified according to the number of pairs M, to their position i_m ($1 \leq i_m \leq L$, $1 \leq m \leq M$) and to the number of unpaired electrons N_m between pairs m and $m+1$. The number of sites between pairs m and $m+1$ is given by $L_m = i_{m+1} - i_m - 1$. Now the essential point is that the subsystem made of N_m unpaired fermions located between pairs m and $m+1$ has the same energy levels as a system of N_m free spinless fermions on a finite chain of length $L_m - N_m - 1$. This can be shown in two steps: (i) there is a one to one correspondence between the states, (ii) the matrix elements of the Hamiltonian are the same after mapping.

The reduction of size is due to the constraint imposed by $V = +\infty$, which implies that two fermions cannot be on nearest-neighbor sites and thus that the number of available configurations is greatly reduced. Now, if we consider the entity made of a fermion and the site right to it as a new particle, the number of available sites is reduced by the number of fermions between the two pairs and by 1 because of the pair at the boundary. For example, if we consider a state where there are seven sites and two fermions between two pairs, there are six configurations and the correspondence reads

$$
\begin{aligned}
|de\uparrow e\downarrow eeede\rangle &\rightarrow |dsseed\rangle', \\
|de\uparrow ee\downarrow eede\rangle &\rightarrow |dsesed\rangle', \\
|de\uparrow eee\downarrow ede\rangle &\rightarrow |dseesd\rangle', \\
|dee\uparrow e\downarrow eede\rangle &\rightarrow |dessed\rangle', \\
|dee\uparrow ee\downarrow ede\rangle &\rightarrow |desesd\rangle', \\
|deee\uparrow e\downarrow ede\rangle &\rightarrow |deessd\rangle',
\end{aligned}
$$

where e, d, and s stand for empty, doubly occupied and single occupied sites. Here the number of sites available for the free fermions is four instead of seven.

Then it is easy to see that these new particles obey the Pauli principle, and that the action of H_0 is to let these new particles hop with an amplitude $-t$ whenever there is a free site next to it. For instance,

$$
\begin{aligned}
H_0|de\uparrow ee\downarrow eede\rangle = -t\Big(&|dee\uparrow e\downarrow eede\rangle \\
&+|de\uparrow e\downarrow eeede\rangle \\
&+|de\uparrow eee\downarrow ede\rangle\Big)
\end{aligned}
\tag{12}
$$

can be translated as

$$
H_0'|dsesed\rangle' = -t(|dessed\rangle' + |dsseed\rangle' + |dseesd\rangle'). \tag{13}
$$

So the energy levels are those of N_m spinless fermions on $L_m - N_m - 1$ sites.

Let us remember that if we have $\tilde{N}$ spinless fermions on $\tilde{L}$ sites with open boundary conditions, then the states can be enumerated by quantum numbers $q = 1, \ldots, \tilde{N}$ with the energies $-2t\cos q\pi/(\tilde{L}+1)$, so that the ground-state energy is given by

$$
E_{\rm sf}(\tilde{L},\tilde{N}) = -2t\sum_{q=1}^{\tilde{N}} \cos\frac{\pi q}{\tilde{L}+1} \tag{14}
$$

$$
= t - t\left(\sin\frac{\tilde{N}+1/2}{\tilde{L}+1}\pi\right)\left(\sin\frac{1}{2}\frac{1}{\tilde{L}+1}\pi\right)^{-1}. \tag{15}
$$

This is equivalent to the result obtained by Bethe ansatz[17] for the energy of spinless fermions with large nearest-neighbor repulsion.

Thus, the lowest energy of the configuration above is given as

$$
E = MU + \sum_i^M E_{\rm sf}(L_i - N_i - 1, N_i). \tag{16}
$$

Now we need to get the configuration of doubly occupied sites for which the energy derived above is the lowest. One can easily check that if we divide a system

of spinless fermions into subsystems, so that the numbers of sites and particles are conserved, the energy will always be higher than that of the original system. Note that this result holds because we are considering open boundary conditions. As a consequence the lowest energy is reached if all the pairs sit together. Hence, the lowest energy for a system having M pairs is given by

$$E = MU - E_{\rm sf}(L-N, N-2M), \tag{17}$$

where we have taken into account the fact that the effective space for the $N-2M$ unpaired fermions is reduced from $L-2M+1$ to $L-2M+1-(N-2M)-1 = L-N$.

In the thermodynamic limit ($L \to \infty$) this is given by

$$E/L = \frac{mn}{2}U - \frac{2}{\pi}(1-n)\sin\pi\frac{n}{1-n}(1-m), \tag{18}$$

where $m = 2M/N$ is the proportion of fermions forming pairs and $n = N/L$ is the density of the fermions.

This energy should be minimized as a function of m. If $U > U_c = -4t\cos\pi n/(1-n)$ the energy is minimized for $m = 0$ and there are no pairs in the system. If $-4t < U < U_c$, the minimum is reached for m given by

$$m = \frac{2n-1}{n} + \frac{1-n}{n}\frac{1}{\pi}\arccos(-U/4t). \tag{19}$$

Finally, when $U < -4t$ the energy is minimal for $m = 1$, which means that all the fermions are paired.

For $n = 1/2$ (quarter-filled system) $U_c = 4t$. Above $4t$ every second site is occupied by one fermion with spin up or down. This would correspond to a filled band in our effective model of spinless fermions. However, if we create a pair, it would cost us an energy U, and we can gain $-4t$ in kinetic energy, since we have created two holes at the top of the filled band each having energy $-2t$ (see Fig. 3). Thus the creation of pairs becomes favorable when $U < 4t$. This estimate is in complete agreement with the value of U_c obtained from Eq. (3) for the charge gap, where $E_0(L,N) = 0$ [Fig. 3(a)], $E_0(L,N+1) = U$ [Fig. 3(b)] and $E_0(L,N-1) = -4t$ [Figs. 3(c) and 3(d)] and $\Delta_c = U-4t$ becomes zero when $U = 4t$. This proves

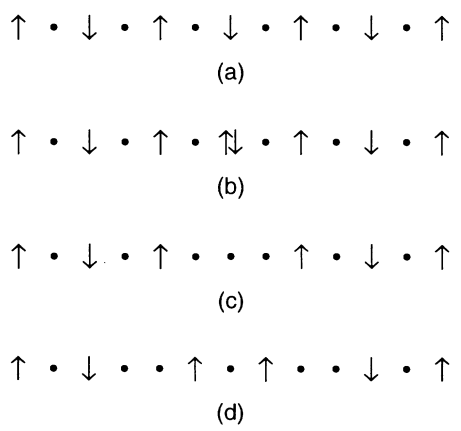

FIG. 3. Typical configuration for N particles on L sites in the $V = +\infty$ limit: (a) $N = L/2$; (b) $N = L/2+1$; (c) and (d) $N = L/2-1$. Dots stand for empty sites.

that $(U,V) = (4t, +\infty)$ is on the boundary of the metal-insulator transition.

Let us now look at the spin gap. When $U < -4t$ we have only local spins in the ground state, and $\Delta_s > 0$. When U becomes larger than $-4t$, paired fermions appear in the ground state. But we saw above that the energy is independent of the spin, which means that $\Delta_s = 0$. So $(U,V) = (-4t, +\infty)$ lies on the boundary of the spin gap.

Finally, it is clear from Eq. (17) that there is phase separation: The ground state consists of a domain of density 1 where all the pairs are packed and a domain of density $< 1/2$ where the unpaired particles can move. So the points $(U,V) = (-4t, +\infty)$ and $(4t, +\infty)$ lie on the boundary of the phase separation.

V. DISCUSSION OF THE LARGE V REGION

The nature of phase (8) is quite puzzling. On the one hand, our numerical results indicate that this phase has no charge gap, no spin gap, and that K_ρ is larger than 1. Then, according to g-ology, the triplet pairing fluctuations should dominate. On the other hand, if we try to understand why this phase might be superconducting, our results concerning the $V = +\infty$ suggest that it is due to the presence of local pairs in the ground state. The argument goes as follows: When $V = +\infty$ and $-4t < U < 4t$, the ground state consists of local pairs that sit together, and of unpaired particles that can move freely (apart from the V interaction) in the part of the sample not occupied by pairs. Then, when V decreases, the pairs start moving around. This can be seen by deriving an effective Hamiltonian in the limit of large but finite V (see Appendix B). The system clearly consists of two types of carriers, local pairs and unpaired particles, that can hop, cross, or exchange. We have not attempted yet a careful study of this effective Hamiltonian. One scenario as to what happens when V decreases is the following. As long as V is not too small, the pressure exerted by the free carriers is sufficient to force the pairs to stay together, and there is still phase separation. However, when V is small enough, the kinetic energy gained by the pairs is comparable to that of the free carriers, and they can move freely in the sample. The ground state is then homogenous and metallic. Superconductivity would then arise from the presence of locals pairs. But these pairs are located on a single site and must be singlet. Then this picture would favor singlet superconductivity, in contradiction to the prediction of g-ology.

Let us note that there is no inconsistency so far. On the one hand, we have not been able to check that the system is a Luttinger liquid when V is large, so that the predictions of g-ology should not be taken too seriously in that region. On the other hand, we have no precise indication that there are still pairs in the ground state when V is so small that we are outside the region of phase separation. In fact, an alternative scenario to that outlined above for the large V case is that the pairs disappear when one leaves the region of phase separation. Instead of having

to reconcile these points of view, it looks more like we have to choose between one of the following possibilities: (i) the system is a Luttinger liquid, there is no pair in the ground state, and the triplet pairing fluctuations dominate; (ii) the system has two types of carriers, local pairs and unpaired particles, it is not a Luttinger liquid, and the singlet pairing fluctuations dominate. How can we choose?

The most natural thing to do would be to look at the low-lying excitations of the system to see whether there are of the Luttinger-liquid type or not. We have indeed tried that, but with no success. For systems as small as 16 sites, it is impossible to say anything by looking at the spectrum directly. There is however an indirect way of testing whether there are pairs in the ground state by studying the response of its ground-state energy to a magnetic flux.

To be more specific, suppose that a closed ring is threaded by a magnetic flux Φ. The units are such that $\Phi = 2\pi$ corresponds to one flux quantum hc/e. This can be taken into account by replacing the kinetic energy by

$$-t\sum_{i,\sigma}(e^{i\Phi/L}c^{\dagger}_{i\sigma}c_{i+1\sigma} + \text{H.c.}), \tag{20}$$

where L is the number of sites. Then, for a noninteracting system the function $f(\Phi)$ defined by $f(\Phi) = \lim_{L\to\infty} L[E_0(\Phi) - E_0(0)]$, where $E_0(\Phi)$ is the ground-state energy for a given flux, is periodic with period 2π. However, if the ground state consists of pairs, as for the negative U Hubbard model, the function $f(\Phi)$ is periodic with period π. If the ground state has both types of carriers, then we expect to be in the intermediate situation where this function is periodic with period 2π but has a local minimum at π.

For finite systems, one finds almost systematically two minima. This is even true in the case of the Hubbard model with repulsive U. The only meaningful information is contained in the limiting behavior when the system size becomes infinite. With systems consisting of 8, 12, and 16 sites, all we can see is the trend. Some results are given in Fig. 4. Quite clearly, when U is negative, but still inside phase (8), the local minimum at π gets deeper when L increases, which suggests that there are pairs in the ground state in the thermodynamic limit. For larger values of U, there is still a well-defined local minimum, but it tends to decrease with the size of the system, so it is impossible to know whether it will survive in the thermodynamic limit.

To summarize what we have learned about phase (8), it seems to us likely that when $U < 0$ there are pairs in the ground state, that the system is not a Luttinger liquid but has a more complicated spectrum including excitations of both the pairs and the unpaired particles, and that it has strong singlet pairing fluctuations. When U becomes positive, the nature of this part of the phase diagram is still very much an open question. There might still be pairs around, so that the whole region has the same behavior, but the pairs might have disappeared as well, in which case the system would be a Luttinger liquid with triplet pairing excitations. More work is needed to settle this issue.

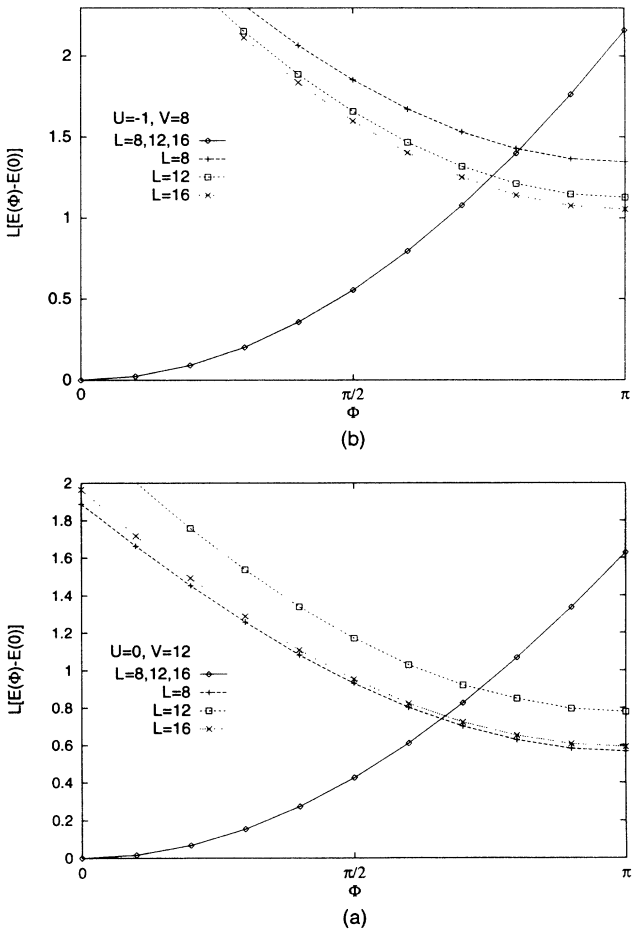

FIG. 4. Ground-state energy as a function of flux for two cases: (a) $U = -1$ and $V = 8$ and (b) $U = 0$ and $V = 12$. The boundary conditions are periodic for $L = 12$ and antiperiodic for $L = 8$ and $L = 16$. The curves having a minimum at $\phi = 0$ are nearly indistinguishble for $L = 8, 12$, and 16, and we have plotted a single set of points.

ACKNOWLEDGMENTS

We acknowledge useful discussions with H. Beck, P. Fazekas, T. Giamarchi, D. Poilblanc, H. Schulz, and X. Zotos. This work was done while both authors were at the University of Neuchatel and was supported in part by the Swiss National Science Foundation under Grants Nos. 20-31125.91 and 20-33964.92.

APPENDIX A: CLUSTER GUTZWILLER APPROXIMATION

The ground-state energy has been estimated with the help of a variational wave function, namely a Gutzwiller-like wave function[18] extended by intersite correlations. That intersite correlations might be essential was first pointed out by Kaplan *et al.*,[19] who showed that the correct $-t^2/U$ energy can be obtained in the case of the half-filled Hubbard model by including the intersite empty doubly occupied correlation in addition to the on-

site correlation. This kind of variational wave function has been applied to different models, and it proved to be useful to get results in regions where other methods have difficulties.

The variational wave function we used can be written

$$|\Psi_{EG}\rangle = \hat{P}|FS\rangle, \tag{A1}$$

where the operator $\hat{P}$ contains the intersite correlations and is given by

$$\hat{P} = \prod_i \prod_{\mu,\nu} [1 - (1 - \lambda_{\mu\nu})\hat{P}_{\mu,i}\hat{P}_{\nu,i+1}]. \tag{A2}$$

The projectors $\hat{P}_{\mu,i}$ at site i are defined by

$$\hat{P}_{\mu,i} = \begin{cases} (1-n_{\uparrow,i})(1-n_{\downarrow,i}) & \text{if } \mu = e, \\ n_{\uparrow,i}(1-n_{\downarrow,i}) & \text{if } \mu = \uparrow, \\ (1-n_{\uparrow,i})n_{\downarrow,i} & \text{if } \mu = \downarrow, \\ n_{\uparrow,i}n_{\downarrow,i} & \text{if } \mu = d. \end{cases} \tag{A3}$$

The $\lambda_{\mu\nu}$'s are the weighting amplitudes of the different nearest-neighbor intersite correlations. For instance, if an empty site and a doubly occupied site are nearest neighbors, the weight of the configuration is multiplied by λ_{ed}. Altogether there are 16 different $\lambda_{\mu\nu}$'s, but they are not independent. Different symmetries, like $\lambda_{\mu\nu} = \lambda_{\nu\mu}$ and zero magnetization, reduce the number of independent weighting amplitudes to 7. Furthermore, the density of particles being given, there are constraints to be satisfied in the minimization process.

The difficult step is to calculate $\langle\Psi_{EG}|H|\Psi_{EG}\rangle$. In general, this cannot be done analytically,[20] and the only "exact" way is to do it with a variational Monte Carlo.[21] There is however an approximate way of calculating this matrix element known as the cluster Gutzwiller approximation[22] which leads to relatively modest numerical tasks, and which has been shown to give very good results on various models. In this scheme, a cluster of four consecutive lattice sites is chosen, and they are labeled by 1, 2, 3, and 4. On this small cluster we can have $4^4 = 256$ different configurations. The weight of each configuration is its weight in the Fermi sea multiplied by the factors λ, and the matrix elements are the matrix elements taken in the Fermi sea multiplied by the amplitudes λ. For instance,

$$\begin{aligned} \langle ed\uparrow\downarrow|ed\uparrow\downarrow\rangle &\to \lambda_{ed}^2\lambda_{d\uparrow}^2\lambda_{\uparrow\downarrow}^2\langle ed\uparrow\downarrow|ed\uparrow\downarrow\rangle_{\mathrm{FS}}, \\ \langle ed\uparrow\downarrow|\hat{A}|ed\uparrow\downarrow\rangle &\to \lambda_{ed}^2\lambda_{d\uparrow}^2\lambda_{\uparrow\downarrow}^2\langle ed\uparrow\downarrow|\hat{A}|ed\uparrow\downarrow\rangle_{\mathrm{FS}}, \\ \langle ed\uparrow\downarrow|\hat{A}|e\uparrow d\downarrow\rangle &\to \lambda_{ed}\lambda_{e\uparrow}\lambda_{d\uparrow}^2\lambda_{\uparrow\downarrow}^2\langle ed\uparrow\downarrow|\hat{A}|ed\uparrow\downarrow\rangle_{\mathrm{FS}}. \end{aligned} \tag{A4}$$

The energy can be obtained by summing the matrix elements of the Hamiltonian over all 256 configurations divided by the norm of the states. However, since the central pairs (2 and 3) and the shell pairs (1 and 2, 3 and 4) are not treated in a symmetric way, the cluster is not homogeneous. In order to force homogeneity, different amplitudes $\lambda_{\mu\nu,s}$ and $\lambda_{\mu\nu,c}$ can be defined for the shell and central pairs. Then Eq. (A4) has to be modified according to

$$\begin{aligned} \langle ed\uparrow\downarrow|ed\uparrow\downarrow\rangle &\to \lambda_{ed,s}^2\lambda_{d\uparrow,c}^2\lambda_{\uparrow\downarrow,s}^2\langle ed\uparrow\downarrow|ed\uparrow\downarrow\rangle_{\mathrm{FS}}, \\ \langle ed\uparrow\downarrow|\hat{A}|ed\uparrow\downarrow\rangle &\to \lambda_{ed,s}^2\lambda_{d\uparrow,c}^2\lambda_{\uparrow\downarrow,s}^2\langle ed\uparrow\downarrow|\hat{A}|ed\uparrow\downarrow\rangle_{\mathrm{FS}}, \\ \langle ed\uparrow\downarrow|\hat{A}|e\uparrow d\downarrow\rangle &\to \lambda_{ed,s}\lambda_{e\uparrow,s}\lambda_{d\uparrow,c}^2\lambda_{\uparrow\downarrow,s}^2\langle ed\uparrow\downarrow|\hat{A}|ed\uparrow\downarrow\rangle_{\mathrm{FS}}, \end{aligned} \tag{A5}$$

and in the minimization procedure we impose the constraint that the densities and correlations are the same everywhere in the cluster. Details can be found in Ref. 22.

Once we have the energy, the inverse compressibility κ^{-1} is easily calculated as

$$\kappa^{-1} = \frac{\partial^2 E}{\partial^2 n}. \tag{A6}$$

We define the point of phase separation to be the point where κ^{-1} vanishes, i.e., where the system becomes unstable against local density fluctuations. A different definition of the phase separation boundary can be given by Maxwell construction.

APPENDIX B: EFFECTIVE HAMILTONIAN FOR LARGE V

In this appendix, we derive an effective Hamiltonian in the limit where the intersite repulsion V is much larger than the on-site interaction U and the hopping t. This can be done by using the Schrieffer-Wolff transformation[23]

$$\begin{aligned} H_{\mathrm{eff}} &= e^{iS}He^{-iS} \\ &= H + i[S,H] - \frac{1}{2}[S,[S,H]] + \cdots. \end{aligned} \tag{B1}$$

We first split the Hamiltonian into two parts, $H = H' + H_{\mathrm{mix}}$, where H' mixes states within a given "Hubbard band," while H_{mix} has matrix elements between different Hubbard bands typically separated by an energy of order U from each other. We can eliminate H_{mix} by choosing S so that

$$H_{\mathrm{mix}} = -i[S,H']. \tag{B2}$$

Then to first order in S

$$H_{\mathrm{eff}} = H' + i\frac{1}{2}[S,H_{\mathrm{mix}}]. \tag{B3}$$

Using standard procedures, the resulting effective Hamiltonian we obtained consists of six parts

$$H_{\mathrm{eff}} = H_0 + H_1 + H_2 + H_3 + H_4 + H_5. \tag{B4}$$

The leading term $H_0 = \mathcal{P}H'\mathcal{P}$ reads

$$H_0 = \mathcal{P}\left[-t\sum_{i,\sigma}\left(c_{i+1,\sigma}^{\dagger}c_{i,\sigma} + \mathrm{H.c.}\right) + U\sum_i n_{i,\sigma}n_{i,-\sigma}\right]\mathcal{P}, \tag{B5}$$

where

$$\mathcal{P} = \prod_{i,\sigma,\sigma'}(1 - n_{i,\sigma}n_{i+1,\sigma'}). \tag{B6}$$

This is a Hubbard model with the additional constraint that two fermions cannot be on neighboring sites.

The remaining H_i's are of order $-t^2/V$. H_1 describes the hopping of pairs

$$H_1 = -2\frac{t^2}{V}\sum_i d_i^\dagger d_i + \text{H.c.}, \tag{B7}$$

where $d_i^\dagger = c_{i,\uparrow}^\dagger c_{i,\downarrow}^\dagger$ ($d_i = c_{i,\downarrow}c_{i,\uparrow}$) is the pair creation (annihilation) operator. Annihilation (creation) of pairs into (from) opposite spin fermions two sites apart is described by

$$H_2 = -\frac{t^2}{V}\sum_i \left(c_{i+1,\uparrow}^\dagger c_{i-1,\downarrow}^\dagger + c_{i-1,\uparrow}^\dagger c_{i+1,\downarrow}^\dagger\right) \times \left(d_{i+1} + 2d_i + d_{i-1}\right) + \text{H.c.} \tag{B8}$$

H_3 describes a pair-electron interchange

$$H_3 = \frac{t^2}{2V}\sum_{i,\sigma} c_{i-1,\sigma}^\dagger d_{i+1}^\dagger d_{i-1} c_{i+1,\sigma} + \text{H.c.} \tag{B9}$$

while H_4 stands for a simultaneous hopping of two fermions

$$H_4 = -\frac{t^2}{V}\sum_i c_{i+2,\sigma}^\dagger c_{i,\sigma} c_{i+1,-\sigma}^\dagger c_{i-1,-\sigma} + \text{H.c.} \tag{B10}$$

Finally, we have a diagonal term

$$H_5 = -\frac{t^2}{6V}\sum_i \Big[(n_{i-1,\uparrow} + n_{i-1,\downarrow} + n_{i+1,\uparrow} + n_{i+1,\downarrow} - 4)^2 + 8\Big]. \tag{B11}$$

* On leave from Research Institute for Solid State Physics, Budapest, Hungary.

[1] J. Solyom, Adv. Phys. **28**, 201 (1979).

[2] V. Emery, in *Highly Conducting One-Dimensional Solids*, edited by J. T. Devrese *et al.* (Plenum, New York, 1979), p. 327.

[3] E. H. Lieb and F. Y. Wu, Phys. Rev. Lett. **20**, 1445 (1968).

[4] P. Wzietek, F. Creuzet, C. Bourbonnais, D. Jérôme, K. Bechgaard, and P. Batail, J. Phys. I (France) **3**, 171 (1993).

[5] B. Dardel *et al.*, Phys. Rev. Lett. **67**, 3144 (1991); B. Dardel, D. Malterre, M. Grioni, P. Weibel, Y. Baer, J. Voit, and D. Jérôme, Europhys. Lett. **24**, 687 (1993).

[6] H. J. Schulz, Phys. Rev. Lett. **64**, 2831 (1990); Int. J. Mod. Phys. B **5**, 57 (1991).

[7] A. Parola and S. Sorella, Phys. Rev. Lett. **64**, 1831 (1990).

[8] A. A. Ovchinnikov, Zh. Eksp. Teor. Fiz. **64**, 342 (1973) [Sov. Phys. JETP **37**, 176 (1973)].

[9] F. Mila and X. Zotos, Europhys. Lett. **24**, 133 (1993) .

[10] G. Spronken, R. Jullien, and M. Avignon, Phys. Rev. B **24**, 5356 (1981).

[11] F. D. M. Haldane, Phys. Rev. Lett. **45**, 1358 (1980); **47**, 1840 (1981); J. Phys. C **14**, 2585 (1981).

[12] For the conformal field theory point of view, see, e.g., H. Frahm and V. E. Korepin, Phys. Rev. B **42**, 10553 (1990), and references therein.

[13] M. Ogata *et al.*, Phys. Rev. Lett. **66**, 2388 (1991).

[14] W. Kohn, Phys. Rev. **133**, A171 (1964).

[15] X. Zotos, P. Prelovsek, and I. Sega, Phys. Rev. B **42**, 8445 (1990).

[16] B. S. Shastry and B. Sutherland, Phys. Rev. Lett. **65**, 243 (1990).

[17] M. Fowler and M. W. Puga, Phys. Rev. B **18**, 421 (1978).

[18] M. C. Gutzwiller, Phys. Rev. **137**, A1726 (1965).

[19] T. A. Kaplan, P. Horsch, and P. Fulde, Phys. Rev. Lett. **49**, 889 (1982).

[20] An exception to that statement can be found in W. Metzner and D. Vollhardt, Phys. Rev. B **37**, 7382 (1988).

[21] See, e.g., H. Yokoyama and H. Shiba, J. Phys. Soc. Jpn. **59**, 3669 (1991).

[22] P. Fazekas, Int. J. Mod. Phys. B **3**, 1765 (1989), P. Fazekas, in *Condensed Matter Theories*, edited by S. Fantoni and S. Rosatti (Plenum Press, New York, 1991), Vol. 6, p. 279.

[23] J. R. Schrieffer and P. A. Wolff, Phys. Rev. **149**, 491 (1966).